Various atomic structures of monolayer silicene fabricated on Ag(111)

Zhi-Long Liu[1], Mei-Xiao Wang[1], Jin-Peng Xu[1], Jian-Feng Ge[1], Guy Le Lay[2], Patrick Vogt[3], Dong Qian[1], Chun-Lei Gao[1], Canhua Liu[1] and Jin-Feng Jia[1]

[1] Key Laboratory of Artificial Structures and Quantum Control (Ministry of Education), Department of Physics and Astronomy, Shanghai Jiao Tong University, Shanghai 200240, People's Republic of China
[2] Aix-Marseille University, CNRS, PIIM UMR 7345, F-13397 Marseille Cedex, France
[3] Technische Universität Berlin, Institut für Festkörperphysik, Berlin, Germany
E-mail: canhualiu@sjtu.edu.cn and jfjia@sjtu.edu.cn

Abstract

Silicene, a monolayer of silicon atoms arranged in honeycomb lattices, can be synthesized on the Ag(111) surface, where it forms several superstructures with different buckling patterns and periodicity. Using scanning tunneling microscopy (STM), we obtained high-resolution images of silicene grown on Ag(111) and revealed its five phases, i.e., $4 \times 4 - \alpha$, $4 \times 4 - \beta$, $\sqrt{13} \times \sqrt{13} - \alpha$, $\sqrt{13} \times \sqrt{13} - \beta$ and $\sqrt{13} \times \sqrt{13} - \gamma$, some observed for the first time. For each of the phases, we have determined its atomic structure by comparing the atomic-resolution STM images with theoretical simulation results previously reported. We thus eliminate the contradictions of previous studies on the structural models of various silicene phases supported by the Ag(111) surface.

Keywords: silicene, Ag(111), scanning tunneling microscope

Silicene is a monolayer of silicon atoms arranged in a two-dimensional (2D) honeycomb structure that is similar to graphene [1], and thus is expected to have essentially very similar electronic properties originated from its unique linear energy-momentum dispersion consisting of massless Dirac fermions [2–5]. Moreover, because of its stronger electron-phonon coupling

and/or spin-orbit coupling, silicene is also expected to be a promising candidate for superconductors [6] and/or topological insulators [7]. In contrast to graphene, however, the preparation of silicene is quite difficult: it cannot be exfoliated from bulk silicon because silicon atoms in the bulk are only sp^3-hybridized while those in silicene are sp^2/sp^3 hybridized [8].

Most experimental studies on silicene have been focused on those synthesized on the Ag (111) surface, although it can be also fabricated on ZrB_2, Ir(111) and MoS_2 surfaces [9–11]. The formation of silicene on Ag(111) is very sensitive to the silicon coverage and annealing temperature in synthesis [12, 13]. Various superstructures with different buckling patterns and periodicity with respect to the Ag(111) substrate, i.e., 4×4 [5, 12–15], $\sqrt{13} \times \sqrt{13}$ [13–18] and $2\sqrt{3} \times 2\sqrt{3}$ [12–14] phases, have been observed by STM. Several groups have performed first principle calculations to understand the atomic and electronic band structures of these buckled silicene phases, in which, however, discrepancies remained. For example, previous experiments with angle-resolved photoemission spectroscopy (ARPES) revealed a linear band dispersion in the 4×4 silicene/Ag(111) phase, indicating the existence of Dirac electrons [5, 19, 20]. However, consequent first principle calculations could not find the Dirac fermion characteristics in the calculated band structure of the 4×4 silicene/Ag(111) phase, but attributed the linear band to the sp bands of bulk Ag [21] or the strong hybridization between Si and Ag [22, 23]. The stable atomic structural models of the 4×4 phase used in the calculations by different research groups are almost identical [5, 15, 24]. In contrast, atomic structural models of the $\sqrt{13} \times \sqrt{13}$ silicene/Ag(111) phase proposed in the calculations are quite different in different research works [13, 15, 16, 21, 24]. Moreover, Guo *et al* [21] recently proposed another metastable structure for the 4×4 phase, which has not been observed yet.

To eliminate the discrepancies in the understanding of the silicene atomic structures on Ag (111), we reinvestigated the 4×4 and $\sqrt{13} \times \sqrt{13}$ phases with STM performed at 77 K. In the obtained high-resolution STM images, we succeeded in observing not only the metastable 4×4 phase for the first time, but also three different $\sqrt{13} \times \sqrt{13}$ phases corresponding to three atomic structural models proposed in previous theoretical reports.

The experiments were performed in a commercial UHV system (Unisoku-USM-1300S3He), which consists of a preparation chamber for sample treatment and an insert chamber for STM observation at low temperature cooled by liquid nitrogen or liquid helium. The base pressure of the whole system is 1×10^{-10} Torr. The Ag(111) single crystal surface was cleaned by Ar$^+$ bombardment (2.0 keV, 5×10^{-5} Torr) and subsequent annealing at ~500 °C for 25 min. Various silicene/Ag(111) phases were fabricated by the deposition of Si atoms onto the Ag(111) surface kept at 210–230 °C for 30–60 min. The prepared samples were transferred to the cooling stage kept at 77 K in the inset chamber for STM observations.

It was reported previously that a large domain of 4×4 silicene/Ag(111) phase can be obtained via precise control of the Si coverage and substrate temperature during the sample growth [5, 12, 13]. In the present work, we found it much easier to make silicene with mixed domains, most of which are 4×4 and/or $\sqrt{13} \times \sqrt{13}$ phases when Si coverage is approximately 1 ML without precise control, as figure 1(a) shows. If the Si deposition is further continued, one would see that both 4×4 and $\sqrt{13} \times \sqrt{13}$ domains shrink while $\sqrt{3} \times \sqrt{3}$ silicene/Ag(111) phase domains come into form (not shown here). It is noted that with only 4×4 and/or $\sqrt{13} \times \sqrt{13}$ phase domains, the silicene sheet does not cross the
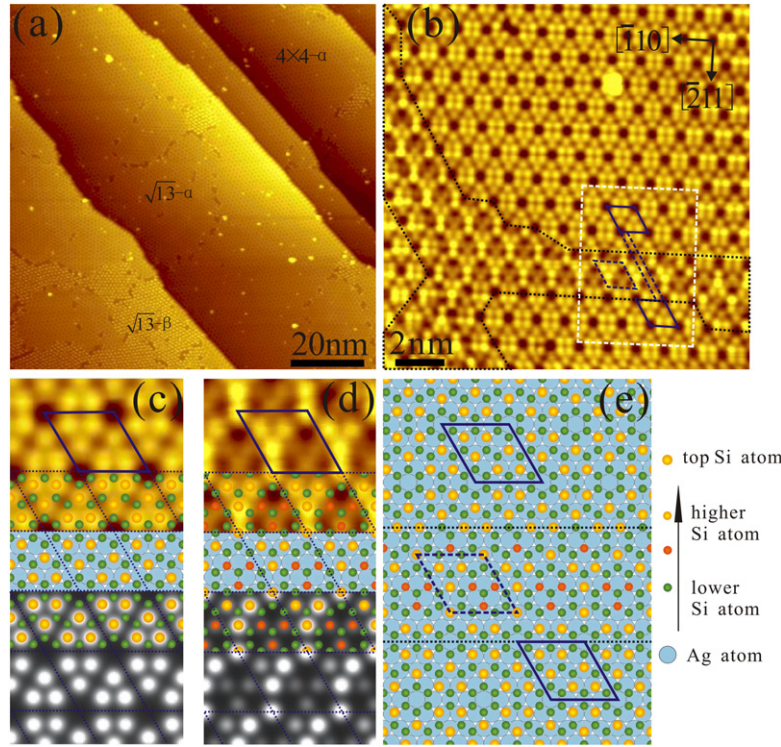
Figure 1. (a) Topography STM image of the silicene/Ag(111) superstructure with various phase domains taken at U = −1.2 V and I = 0.1 nA. (b) High-resolution STM image taken on 4×4 phase domains at U = 115 mV and I = 0.2 nA. Rhombuses superimposed on the image indicate the 4×4 unit cells. Dotted lines indicate the boundaries between two 4×4 phase domains. (c) and (d) Enlarged STM images of 4×4−α and 4×4−β phases taken at U = 5 mV and U = −115 mV, respectively. In both images, the size is $3.05 \times 2.63 \, \text{nm}^2$ and I = 0.2 nA. Below the STM images are STM simulation results previously calculated and based on the ball models superimposed thereon, after [5, 21]. (e) Ball structural model for the area indicted by the white dashed rectangle in (b).

substrate steps. This is why we always have very sharp steps in the STM images, as figure 1(a) shows.

With low sample bias, it is easy to obtain atomic-resolution STM images of the silicene phases on Ag(111), as shown in figure 1(b). Two major 4×4 domains having unit cells represented by two solid rhombuses are visible in the figure. These two domains have a lateral shift from each other in the $\left[01\bar{1} \right]$ direction, as the black dashed lines indicate, resulting in a narrow domain boundary, which consists of another 4×4 phase domain with the unit cell indicated by the dashed rhombus in the figure. Enlarged STM images of the major and minor 4×4 phases are shown in figures 1(c) and (d), respectively. Obviously, these two 4×4 phases show totally different contrast variations in the STM images. We denote them hereafter by 4×4−α and 4×4−β phases, respectively.

The STM image of the 4×4−α phase agrees well with those of 4×4 silicene/Ag(111) phase reported in previous STM studies. Its commonly accepted atomic structure is exhibited in a ball model superimposed on the STM image as well as on its STM simulation result [5] shown

in figure 1(c). In each unit cell there are 18 silicon atoms, six of which locate a little higher away from the top Ag layer and thus present in six bright protrusions with identical brightness in STM images.

It is noted that the $4 \times 4 - \beta$ phase revealed here has not been observed previously. A recent calculation study [21] demonstrated that the 4×4 silicene/Ag(111) phase may have a metastable structure that is different from the stable one in the buckling pattern as well as the adsorption site despite of that both of them have the Si honeycomb structure with a same in-plane size. The lower panel of figure 1(d) shows the simulation result of the metastable 4×4 structure obtained in the previous calculations and its superimposed ball model [21]. It is easy to find in figure 1(d) that the previous STM simulation result resembles our STM images very well: one bright protrusion sits at the corner of the 4×4 unit cell and six within it with different contrast variations. The resemblance of the STM image to the simulation result implies strongly that the $4 \times 4 - \beta$ phase found in our experiment is the metastable structure of the 4×4 silicene/Ag(111) phase proposed in the previous theoretical study. Another fact supporting this idea is that the $4 \times 4 - \beta$ phase domain is always found only in a very limited area in between two $4 \times 4 - \alpha$ phase domains, indicating that the former phase is less stable than the latter one, in consistence with the previous calculation result that the cohesive energy E_c in the $4 \times 4 - \alpha$ phase is 4 (meV Si^{-1} atom) higher than that of $4 \times 4 - \beta$ [21]. It is worth emphasizing that the $4 \times 4 - \beta$ phase found in the STM observations is intrinsically a domain structure and its formation is mainly due to the one-quarter-period shift of two $4 \times 4 - \alpha$ phase domains. Following the ball structural models of figures 1(c) and (d), we succeeded in reproducing the STM image containing both two $4 \times 4 - \alpha$ domains and their domain boundary structure, i.e, $4 \times 4 - \beta$, as figure 1(e) shows.

Another well studied silicene phase on Ag(111) is $\sqrt{13} \times \sqrt{13}$ with a rotational angle of $\pm 13.9°$ with respect to $\left[1\bar{1}0 \right]$ direction of the Ag(111) substrate, as schematically illustrated in figure 2(h). Several research groups have proposed various atomic structural models for the $\sqrt{13} \times \sqrt{13}$ phase [13, 15, 16, 21, 24], as summarized in figure 2. We name these structural models by Model A, Model B, and so on hereafter. It is noted that we redraw the ball models after the previous reports without performing any symmetry operation, which can actually give 4 symmetry equivalent $\sqrt{13} \times \sqrt{13}$ structures [25]. Brighter balls correspond to Si atoms located higher away from the Ag top layer. In figure 2, below each ball model, STM simulation results are shown, except in figure 2(g), since, in that case, no simulation result has been reported. To easily learn the similarities and differences among these structural models, we put those with the rotational angle of $+13.9°$ from $\left[1\bar{1}0 \right]_{Ag}$ in figures 2(a)–(d), while those with $-13.9°$ in figures 2(e)–(g), corresponding to the upper and lower schematic illustrations in figure 2(h), respectively. First of all, one can easily notice that Model D is totally different from the others in Si coverage: it has 18 Si atoms in the unit cell while all the others have 14.

Basically, all of the $\sqrt{13} \times \sqrt{13}$ structural models shown in figure 2 are constructed in a similar way: putting a buckled Si honeycomb sheet onto the Ag(111) surface. The differences among these models are the buckling patterns of the Si sheet itself and its Si adsorption sites on the Ag(111) surface. For example, one can observe that some Si atoms sit exactly on top sites of the Ag(111) substrate in Models A, B, E and F [see the four corners of the rhombuses in the corresponding figures of figure 2], but such are never found in Models C and G. The latter two models are also clearly different from each other both in buckling patterns and Si adsorption
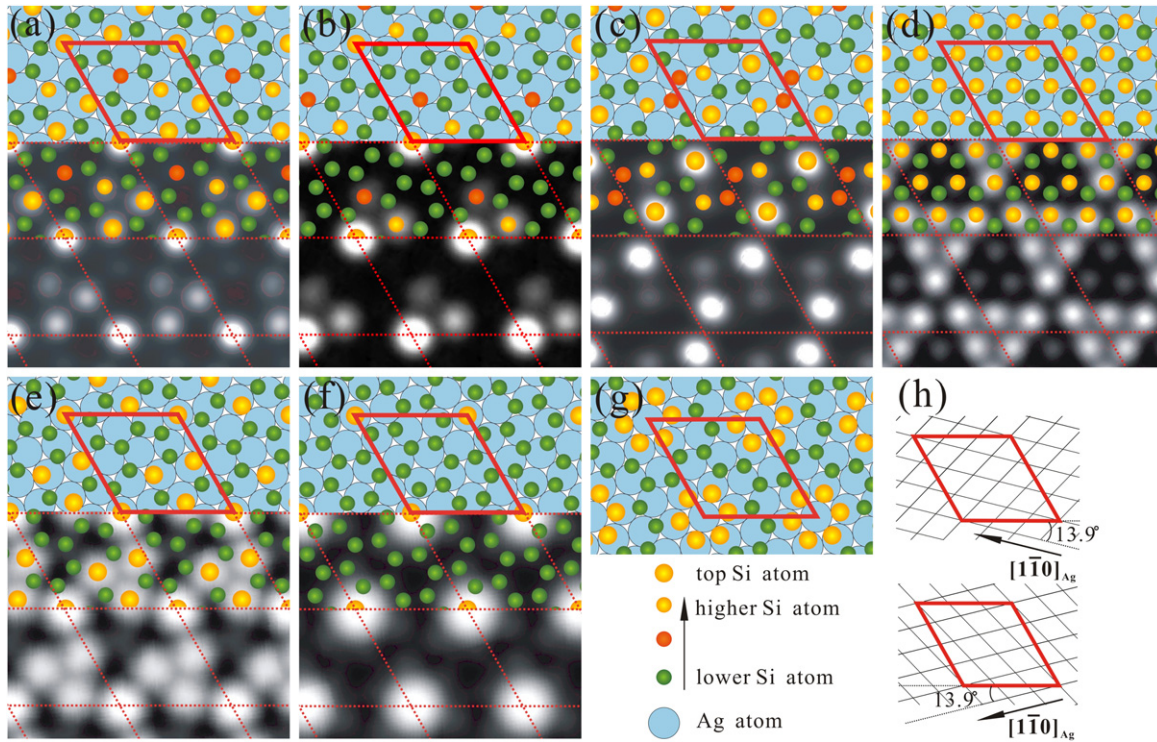
Figure 2. Summary of the atomic structural models proposed previously for the $\sqrt{13} \times \sqrt{13}$ silicene/Ag(111) superstructure. Below each ball model is its corresponding STM simulation result with partial superimposition. (a) and (c) are after [21], (b) after [24], (d) after [15], (e) and (f) after [16], and (g) after [13]. (h) Schematic illustration showing two sets of $\sqrt{13} \times \sqrt{13}$ unit cell with rotational angles of ±13.9° from the $\left[1\bar{1}0\right]_{Ag}$ direction.

sites. It is interesting to note that the similarity among Models A, B, E and F is very high by considering symmetry operations. Actually, the lateral positions of Si atoms with respect to the Ag(111) surface in Models A and E are identical while those in Models B and F are also identical. Both differences between Models A and E and between Models B and F are in their buckling patterns, i.e., the variation of the adsorption height of Si atoms. The difference in the buckling pattern between Models A and E is small, and their STM simulation results appear very similar. In contrast, the STM simulation results of Models B and F appear quite different.

To find out which structural model shown in figure 2 is more appropriate, we have taken atomic-resolution STM images on $\sqrt{13} \times \sqrt{13}$ domains at various sample bias, and show the results in figures 3(a)–(d), where a 4×4 domain is also visible. On the central right part of the STM image in figure 3(a), one can see a small domain of the $\sqrt{13} \times \sqrt{13}$ phase determined from its unit cell size and its rotational angle with respect to the 4×4 domain, as indicated by the blue rhombus and lines, respectively. On the upper part of the same STM image [figure 3(a)], another domain contains many large bright protrusions arranged in a hexagonal pattern with the unit cell indicated by the red rhombus. A previous STM study has reported similar large bright protrusions and attributed them to a 3.5×3.5 phase [17]. Here, however, we found the separation of the nearest-neighbor bright protrusions is 1.026 nm, corresponding to
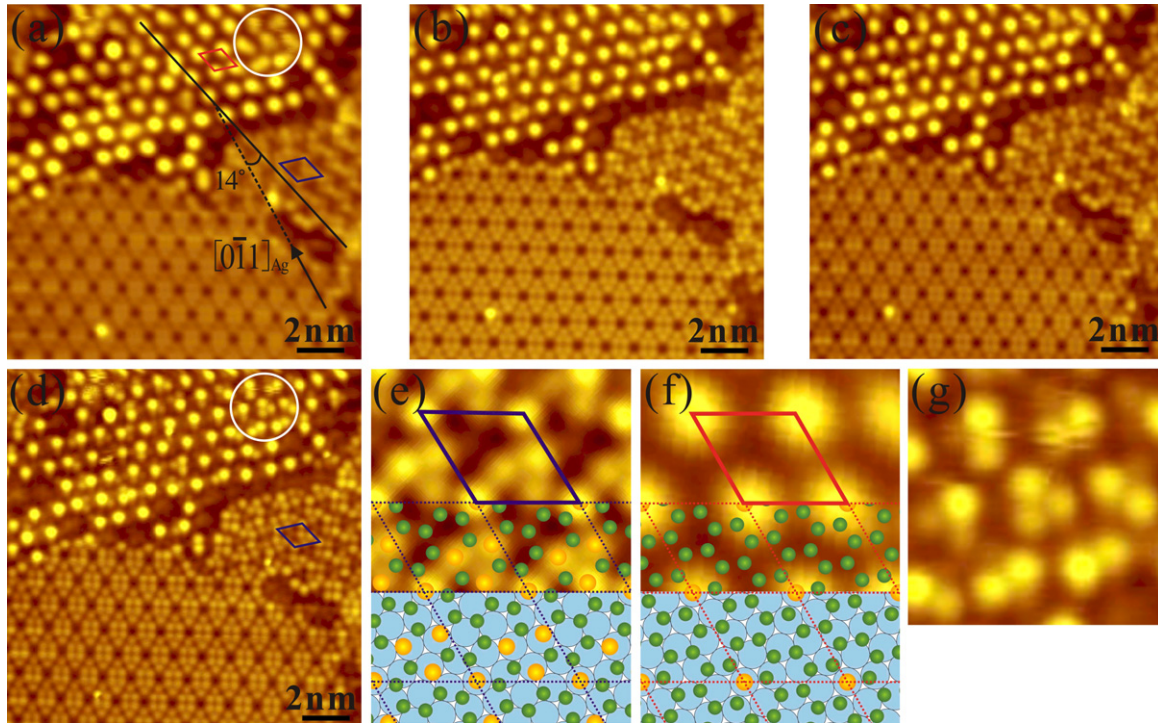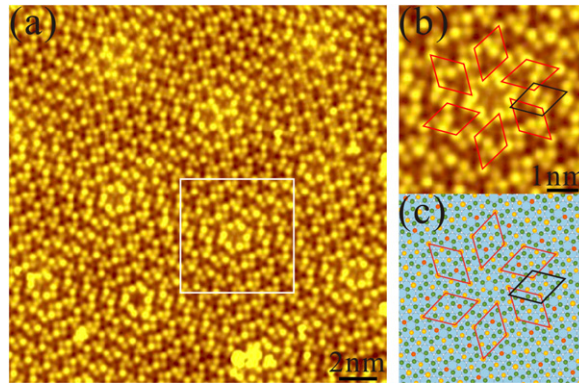
Figure 3. (a)–(d) High-resolution topography STM images of silicene/Ag(111) superstructure taken at sample bias of (a) −1.2 V, (b) −50 mV, (c) −20 mV and (d) −1 mV and I = 0.2 nA for all images. (e) and (f) are enlarged STM images of $\sqrt{13} \times \sqrt{13} - \alpha$ and $\sqrt{13} \times \sqrt{13} - \beta$ cut from (d) and (a), respectively. The ball models below (e) and (f) are the same as those in figures 2(e) and (e), respectively. (g) An enlarged STM image cut from (d), showing the area indicated by the circle.

$\sqrt{13}\,a$ but not 3.5a, where a = 0.289 nm is the lattice constant of the Ag(111) 1 × 1 surface. Moreover, the lattice of the bright protrusions has a rotational angle of ∼14° with respect to the 4 × 4 lattice, as the black lines indicate in figure 3(a). Based on these observations, we attribute the bright protrusions observed here to another $\sqrt{13} \times \sqrt{13}$ phase, and denote the former and later by $\sqrt{13} \times \sqrt{13} - \alpha$ and $\sqrt{13} \times \sqrt{13} - \beta$, respectively.

The STM images of the $\sqrt{13} \times \sqrt{13} - \alpha$ phase taken at high sample bias, as shown in figure 3(a), are consistent with those reported previously [13, 15, 17]. By lowering the sample bias, we can obtain very distinct atomic-resolution STM images of the $\sqrt{13} \times \sqrt{13} - \alpha$ phase, as figures 3(b)–(d) show. Figure 3(e) shows a zoom-in, which appears very similar to the STM simulation results shown in figures 2(e) and (a) when crystal symmetry is considered. Although only Model E is drawn in figure 3(e) to help comparing, it is worth noting that Model A may be also appropriate for the $\sqrt{13} \times \sqrt{13} - \alpha$ phase since both of their simulation results reproduce the STM images very well.

On the $\sqrt{13} \times \sqrt{13} - \beta$ phase domain, each unit cell contains one bright protrusion in its high-sample-bias STM images, as figure 3(a) shows. A recent STM study reported a similar $\sqrt{13} \times \sqrt{13}$ domain consisting of the bright protrusions and proposed a structural model, which is very similar to Model F, for it [18]. However, perusal on figure 3(a) reveals that the

Figure 4. (a) High-resolution topography STM image taken on a $\sqrt{13} \times \sqrt{13}$ domain showing a large hexagonal pattern. $U = 3\,mV$ and $I = 0.2\,nA$. (b) Enlarged STM image cut from the square indicated in (a). (c) Ball structural model for the vortex pattern shown in (b). It is based on the models shown in figures 2(a) and (c).

bright protrusions are not completely identical: some are very round while some are elongated. Several elongated protrusions are indicated by the white circle in figure 3(a). In the STM images taken at very low biases, as figures 3(c) and (d) show, the bright protrusions shrink in size and some surrounding substructures become visible. The elongated protrusions observed at high bias split into two or three smaller protrusions in the STM images taken at low bias, as the circle indicates in figure 3(d) and as also shown in the zoomed-in image in figure 3(g). These STM observations imply that the $\sqrt{13} \times \sqrt{13} - \beta$ phase should have a nonuniform atomic structure. Actually, the single-protrusion and triplet-protrusion STM images shown in figures 3(f) and (g) appear very similar to the STM simulation results based on Models F and B, respectively. Considering that these two structural models have the same in-plane atomic arrangement and differ only in buckling patterns, it is reasonable to believe that the $\sqrt{13} \times \sqrt{13} - \beta$ phase has a uniform in-plane atomic arrangement as Models F and B proposed, but lacks long range order in its buckling pattern. It is the limited buckling disorder that corresponds to the nonconformity of the bright protrusions observed in the STM images of the $\sqrt{13} \times \sqrt{13} - \beta$ phase domains.

In the course of our experiments, we could always find more domains of the $\sqrt{13} \times \sqrt{13} - \alpha$ phase than those of the $\sqrt{13} \times \sqrt{13} - \beta$ phase, indicating that the former phase should be more stable than the latter one. Concerning to this $\sqrt{13} \times \sqrt{13} - \alpha$ phase, another interesting feature was observed in our STM measurements: the $\sqrt{13} \times \sqrt{13} - \alpha$ domains are in triangular shapes and thus form a large hexagonal pattern with a side length of about $5\sqrt{13}\,a$, as figure 4(a) shows. Although the large hexagonal pattern has no long range order, one can still easily recognize its vortices, one of which, for example, is located at the center of the white square traced on the STM image in figure 4(a).

Figure 4(b) shows the enlarged STM image of the vortex surrounded by six $\sqrt{13} \times \sqrt{13} - \alpha$ unit cells, as the red rhombuses indicate. Each domain boundary of two adjacent $\sqrt{13} \times \sqrt{13} - \alpha$ domains consists of a chain of tetramer protrusions. It is interesting to find that the tetramers, as the black $\sqrt{13} \times \sqrt{13}$ rhombus indicates in figure 4(b), appear very similar to that in the STM simulation result of Model C shown in figure 2(c). In both tetramers of the STM and the simulation results, one pair of the diagonal protrusions are brighter than the

other pair, which strongly indicates that the chains of the tetramer protrusions between two $\sqrt{13} \times \sqrt{13} - \alpha$ domains have the atomic structure as Model C proposed in figure 2(c). We name the domains of the tetramer chains as the $\sqrt{13} \times \sqrt{13} - \gamma$ phase.

In the previous calculation results, Model C was a metastable structure with respect to Model A; both models were proposed by Guo *et al* [21]. This is consistent with our STM observations that the $\sqrt{13} \times \sqrt{13} - \gamma$ phase always forms at domain boundaries of the $\sqrt{13} \times \sqrt{13} - \alpha$ phase, indicating that the latter phase is more stable than the former one. To understand the Si atomic arrangement of the vortex pattern observed by STM, Si atoms are put on the Ag(111) surface following the $\sqrt{13} \times \sqrt{13}$ ball models of A and C, as figure 4(c) shows. With the $\sqrt{13} \times \sqrt{13}$ rhombuses superimposed thereon, one can see that Model C is constructed between two, and Model A just upon changing the buckling pattern without changing the Si honeycomb structure.

In summary, we have studied with STM monolayer silicene sheets supported by a Ag(111) substrate and revealed in high-resolution images that silicene has various buckling patterns, more than observed in previous experiments. Newly observed metastable $4 \times 4 - \beta$ and $\sqrt{13} \times \sqrt{13} - \gamma$ phases are found to form at domain boundaries of the $4 \times 4 - \alpha$ and $\sqrt{13} \times \sqrt{13} - \alpha$ phases, respectively. In addition, we discovered a $\sqrt{13} \times \sqrt{13} - \beta$ phase that has no long range order in its buckling pattern. All of these STM observations can be well explained by using a few previously proposed structural models of the 4×4 and/or $\sqrt{13} \times \sqrt{13}$ silicene/Ag(111) phases, namely those by Guo Z X *et al* [21]. As a consequence, the controversies in previous calculation results are largely eliminated.

Acknowledgements

References

[1] Geim A K and Novoselov K S 2007 The rise of graphene *Nature Mater.* **6** 183
[2] Takeda K and Shiraishi K 1994 Theoretical possibility of stage corrugation in Si and Ge analogs of graphite *Phys. Rev.* B **50** 14916
[3] Guzmán-Verri G G and Lew Yan Voon L C 2007 Electronic structure of silicon-based nanostructures *Phys. Rev.* B **76** 075131
[4] Chen L *et al* 2012 Evidence for dirac fermions in a honeycomb lattice based on silicon *Phys. Rev. Lett.* **109** 056804

[5] Vogt P *et al* 2012 Silicene: compelling experimental evidence for graphenelike two-dimensional silicon *Phys. Rev. Lett.* **108** 155501

[6] Chen L, Feng B J and Wu K H 2013 Observation of a possible superconducting gap in silicene on Ag(111) *Appl. Phys. Lett.* **102** 081602

[7] Liu C C, Feng W X and Yao Y G 2011 Quantum spin hall effect in silicene and two-dimensional germanium *Phys. Rev. Lett.* **107** 076802

[8] Houssa H, Pourtois G, Afanas'ev V V and Stesmans A 2010 Can silicon behave like graphene? a first-principles study *Appl. Phys. Lett.* **97** 112106

[9] Fleurence A *et al* 2012 Experimental evidence for epitaxial silicene on diboride thin films *Phys. Rev. Lett.* **108** 245501

[10] Meng L *et al* 2013 Buckled silicene formation on Ir(111) *Nano Lett.* **13** 685

[11] Chiappe D *et al* 2014 Two-dimensional Si nanosheets with local hexagonal structure on a MoS_2 surface *Adv. Mater.* **24** 2096

[12] Feng B J *et al* 2012 Evidence of silicene in honeycomb structures of silicon on Ag(111) *Nano Lett.* **12** 3507

[13] Jamgotchian H *et al* 2012 Growth of silicene layers on Ag(111): unexpected effect of the substrate temperature *J. Phys.: Condens. Matter.* **24** 172001

[14] Chiappe D, Grazianetti C, Tallarida G, Fanciulli M and Molle A 2012 Local electronic properties of corrugated silicene phases *Adv. Mater.* **24** 5088

[15] Lin C L *et al* 2012 Structure of silicene grown on Ag(111) *Appl. Phys. Express* **5** 045802

[16] Enriquez H, Vizzini S, Kara A, Lalmi B and Oughaddou H 2012 Silicene structures on silver surfaces *J. Phys.: Condens. Matter.* **24** 314211

[17] Arafune R *et al* 2013 Structural transition of silicene on Ag(111) *Surf. Sci.* **608** 297

[18] Tchalala M R *et al* 2014 Atomic and electronic structures of the $(\sqrt{13} \times \sqrt{13})$R13.9° of silicene sheet on Ag (111) *Appl. Surf. Sci.* **303** 61–6

[19] Tsoutsou D, Xenogiannopoulou E, Golias E, Tsipas P and Dimoulas A 2013 Evidence for hybrid surface metallic band in (4×4) silicene on Ag(111) *Appl. Phys. Lett.* **103** 231604

[20] Avila J *et al* 2013 Presence of gapped silicene-derived band in the prototypical (3×3) silicene phase on silver (111) surfaces *J. Phys.: Condens. Matter.* **25** 262001

[21] Guo Z X, Furuya S, Iwata J I and Oshiyama A 2013 Absence and presence of dirac electrons in silicene on substrates *Phys. Rev.* B **87** 235435

[22] Cahangirov S *et al* 2013 Electronic structure of silicene on Ag(111): strong hybridization effects *Phys.* B **88** 035432

[23] Yuan Y *et al* 2014 Strong band hybridization between silicene and Ag(111) substrate *Physica* E **58** 38–42

[24] Gao J F and Zhao J J 2012 Initial geometries, interaction mechanism and high stability of silicene on Ag(111) surface *Sci. Rep.* **2** 861

[25] Resta A *et al* 2013 Atomic structures of silicene layers grown on Ag(111): scanning tunneling microscopy and noncontact atomic force microscopy observations *Sci. Rep.* **3** 2399